Supramolecular Assembly of In-Plane Organic Crystals via Solvent-Vapor Exposure

Debra J. Mascaro[1] and Vladimir Bulović[2]

[1]Department of Mechanical Engineering, University of Utah, Salt Lake City, UT 84117
[2]Department of Electrical Engineering, Massachusetts Institute of Technology, Cambridge MA, 02139

Abstract

The exceptional electronic and optical properties of high-quality organic crystals are well known and have been exploited in active electronic and optoelectronic devices such as field-effect transistors, photodetectors and optical modulators. This paper describes a room temperature method for in-plane growth of organic crystal needles from initially amorphous thin films of the molecular organic semiconductor tris(8-hydroxy-quinoline)aluminum (Alq_3). Vacuum-deposited Alq_3 films are exposed to methanol vapor at room temperature and pressure, yielding submicron-thick needles with typical in-plane dimensions of several microns wide by tens of microns long. This paper presents characterization results and discusses the mechanisms of crystal growth.

Keywords: Organic optoelectronics, Organic single crystals, Crystal growth, Solvent-vapor annealing.

1. Introduction

The challenge of generating crystals of organic materials has been pursued by many research groups who aim to develop materials sets for active electronic and optoelectronic devices. The growth of free-standing organic crystals millimeters in size has been previously demonstrated by resublimation and solvent recrystallization [1], and in a few studies discrete active devices have been fabricated using such crystals [2-4]. However, in order to enable monolithic integration of active organic components into all-organic or hybrid integrated systems, it is necessary to form organic crystals in the plane of a large area (cm^2) substrate.

The deposition of high purity molecular organic materials onto planar substrates is most often accomplished by vacuum sublimation, but the deposited thin films are typically amorphous or at best polycrystalline with grain sizes on the scale of microns. Elevated substrate temperatures have been used to improve crystallinity or select a particular crystalline phase during vacuum deposition [5]. In addition, post-deposition thermal treatment, solvent exposure, and solvent-vapor exposure have been shown to induce grain growth as well as amorphous-to-crystalline or polymorphic transformations in molecular organic thin films [6-9]. Previous solvent-vapor studies have typically focused on organic systems of low solubility and high tendency to crystallize. In this study, the ready solubility of Alq_3 in methanol enables the formation of much larger crystals despite the fact that Alq_3 is typically exploited (e.g. in organic light-emitting devices) for its low tendency to crystallize.

The crystal formation method is demonstrated using Alq_3 since it is among the most extensively studied molecular organic semiconductors. Vacuum-sublimed amorphous thin films of Alq_3 have been shown to be morphologically stable under inert atmosphere and room temperature conditions [10], but thermal annealing above the Alq_3 glass transition temperature (T_g=175 °C [11]) results in the formation of micron-scale disk-like clusters of crystals [12]. Vacuum evaporation of Alq_3 onto heated glass substrates pre-rubbed with polytetrafluoroethylene (PTFE) has also been shown to yield polycrystalline Alq_3 films of planar ~1-2 micron crystallites [13].

Similar to thermally-assisted crystallization of Alq_3, exposure of Alq_3 films to acetone vapor was reported to yield micron-scale crystallized regions [14]. Moreover, we previously demonstrated the formation of millimeter-scale Alq_3 crystalline needles via chloroform-vapor exposure of amorphous Alq_3 films on chemically-modified submicron surface-relief gratings [15]. Both the surface chemistry and surface-relief were instrumental in the reorganization of Alq_3 to form elongated crystal needles aligned parallel to the grating direction [16]. The results reported here are simpler in that exposure to methanol vapor yielded large in-plane crystals without the need for surface modification or substrate patterning.

2. Experimental

Silicon or glass substrates were cleaned via the following steps: ultrasonication in dilute detergent,

deionized water, and acetone; immersion in boiling 1,1,1-tricloroethane; ultrasonication in acetone; immersion in boiling 2-propanol. The substrates were then dried in a stream of nitrogen and further cleaned by UV-ozone treatment for 5 minutes. 10-20 nm thick films of Alq_3 were thermally evaporated in vacuum ($<10^{-6}$ Torr) onto room temperature substrates at rates of 0.1-0.3 nm/s as measured by a quartz crystal thickness monitor.

Following the evaporation of Alq_3, the substrates were placed in a glass jar together with a beaker of methanol, and the jar was sealed with a Teflon-lined cap. Exposure times ranged from several minutes to several days. The dimensions of the Alq_3 needles formed via methanol-vapor exposure were characterized by optical microscopy (needle length) and atomic force microscopy (AFM) (needle width, thickness). Optical properties of the needles were investigated via fluorescence microscopy and confocal microscopy (365 nm excitation wavelength).

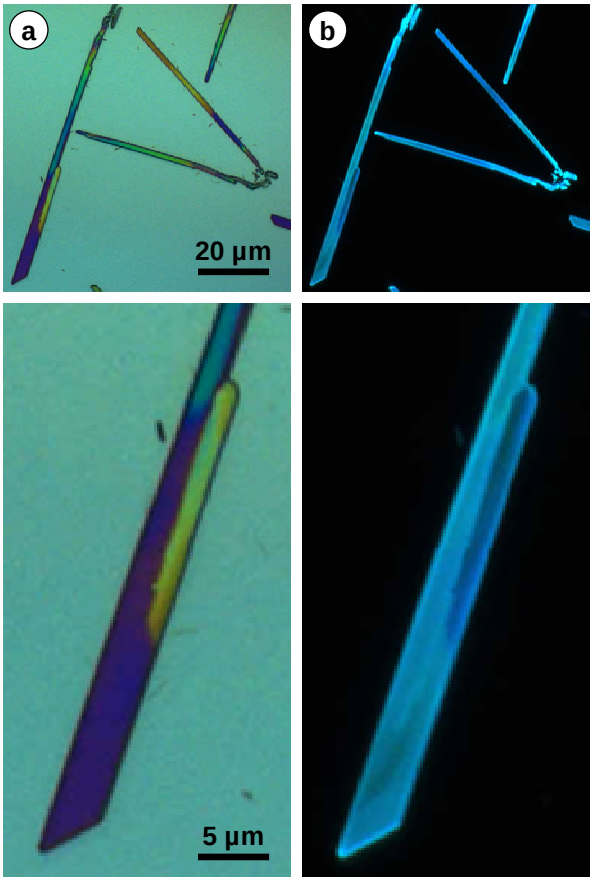

Fig. 1: (a) Optical and (b) corresponding fluorescence micrographs (λ_{exc}=365 nm) of Alq_3 crystalline needles on a silicon substrate. The needles formed from a 15 nm thick Alq_3 film during exposure to methanol vapor for 200 minutes.

3. Results

Exposure of the Alq_3 thin films to methanol vapor results in the formation of crystalline Alq_3 needles such as those shown in the Fig. 1 optical and fluorescence micrographs for a 200 minute exposure. Based on AFM measurements, the needles are a few hundred nanometers thick; the colors observed in the optical micrographs are good indicators of needle thickness – i.e. the yellow portion of the needle in Fig. 1c is ~550 nm thick, while the blue region is ~450 nm thick. As such, the crystal thickness exceeds the initial amorphous film thickness by as much as a factor of 50. After extended exposures the needles achieve in-plane dimensions of a few microns wide by tens of microns long, with typical thickness:width:length ratios of 1:10:200.

Distinct facets are observed at the Alq_3 needle ends and at locations of abrupt thickness change, indicative of crystallinity (Fig. 1). While some needles display a gradual change in thickness, others are uniformly thick over the entire length. The overall optical smoothness of the needle faces is evidenced in fluorescence micrographs that show waveguiding of the Alq_3 fluorescence with outcoupling occurring at needle edges and defects (Fig. 1b). Polarized fluorescence measurements show a change in photoluminescence (PL) intensity with polarization angle. Fig. 2 plots the normalized PL intensity (365 nm excitation wavelength) as a function of polarizer angle for several crystalline needles on two separate substrates, where zero degrees corresponds to the

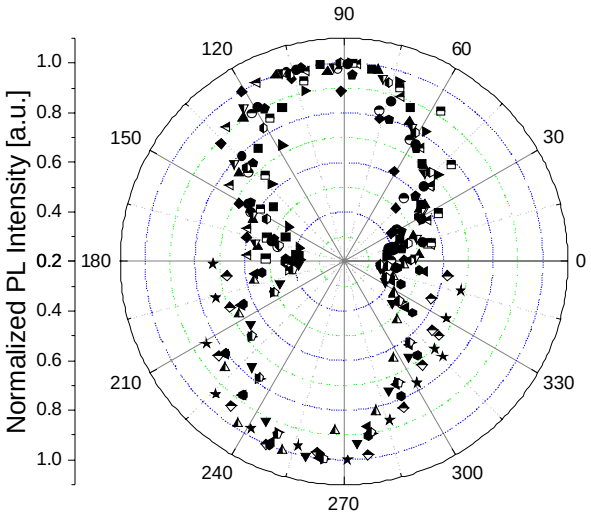

Fig. 2: Normalized PL intensity (λ_{exc}=365 nm) as a function of polarizer angle for several crystalline needles on substrates from two separate experiments. Zero degrees corresponds to the polarizer aligned with the long axis of the needle.

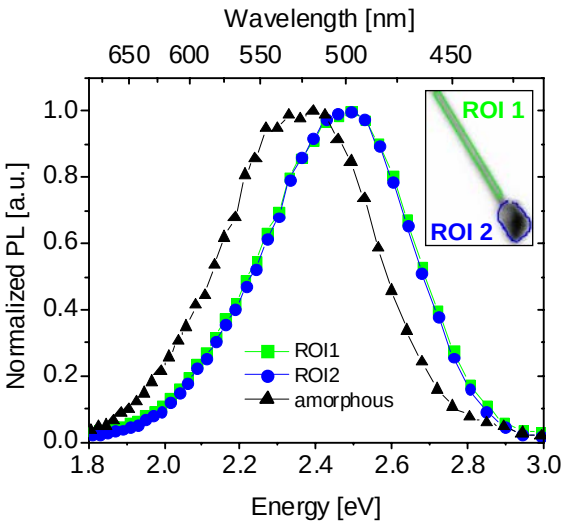

Fig. 3: PL spectra of an Alq_3 crystalline needle formed during methanol-vapor exposure and an (as-deposited) amorphous Alq_3 thin film, obtained via confocal microscopy (λ_{exc}=365 nm). Spectra are plotted for both "regions of interest" shown in the inset PL intensity image.

polarizer aligned with the needle long axis. The two lobes in the polar plot correspond to two crystal populations having different orientations of the transition dipole relative to the needle long axis.

PL spectra corresponding to an amorphous Alq_3 thin film and an Alq_3 needle formed during exposure to methanol vapor are shown in Fig. 3. The spectra were generated via confocal microscopy (365 nm excitation wavelength) by performing a sequence of scans with narrow collection windows. The spectra obtained from the two "regions of interest" identified in the Fig. 3 inset are identical but blue-shifted by ~30 nm relative to the PL of the as-deposited amorphous film. The observed blue-shift is possibly due to the presence of methanol within the Alq_3 crystals, as blue-shifted PL has previously been reported for clathrated Alq_3(MeOH) crystals [17]. This is in contrast to Alq_3 needles formed during exposure to chloroform vapor which do not exhibit a shift in PL [15].

The AFM images and optical micrographs in Fig. 4 illustrate the morphological progression from a continuous, amorphous Alq_3 nanofilm (not shown) to isolated, in-plane crystals via exposure to methanol vapor. Initially the Alq_3 dewets from the substrate and aggregates to form submicron clumps of Alq_3. After 5 minutes, for example, substrate coverage drops to ~55%, and ~200 nm diameter clumps of ~100 nm maximum thickness are observed amidst remnants of the original film (Fig. 4a). An additional 5 minutes further reduces coverage to ~40% and yields clumps as thick as 250 nm, some of which appear to be

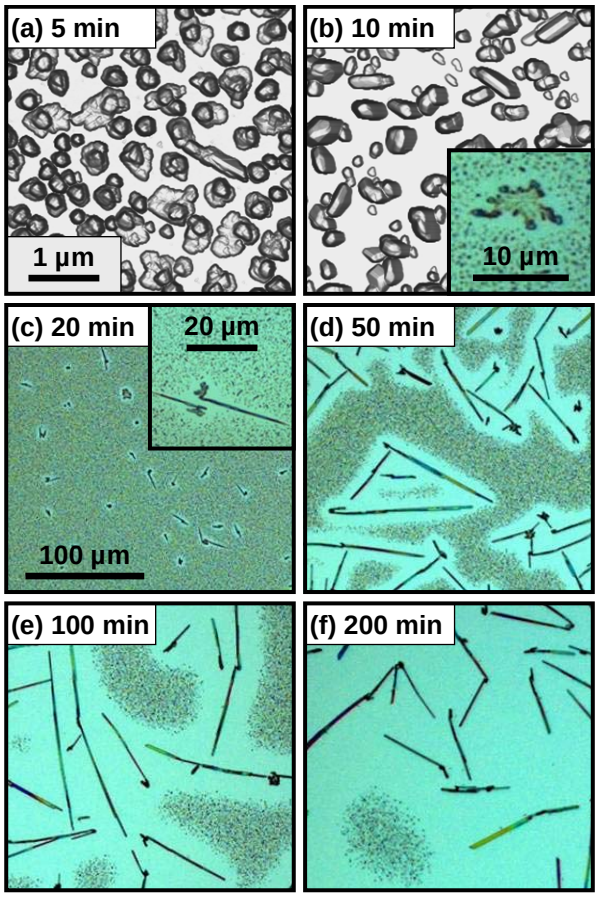

Fig. 4: AFM height images (a, b) and optical micrographs (b inset, c-f) showing the structural evolution of Alq_3 thin films when exposed to methanol vapor for increasing times.

crystalline (Fig. 4b). The 10 minute sample is also decorated with much larger (~10 µm), irregularly-shaped aggregates (Fig. 4b inset) from which the larger crystalline needles appear to grow (Fig. 4c). After exposure for 20 minutes, the substrate remains speckled with Alq_3 clumps except in small regions surrounding individual needles. As the needles grow with increased exposure time, the cleared regions surrounding the needles increase in area (Fig. 4d and 4e) until eventually nearly all of the Alq_3 is incorporated into the needles (Fig. 4f).

4. Discussion

Previous reports of solvent-vapor annealing molecular organic thin films focused on metal phthalocyanines [6-8] and perylene derivates [9], where the goal was to improve photoactivity for xerography and photovoltaic applications. The films tended to have low solubility in the annealing solvents, such that exposure to solvent vapor was presumed to yield a saturated solvent

solution on the film surface. Polymorphic and amorphous-to-crystalline transitions were respectively attributed to solvent-induced relaxation of a metastable crystal phase and increased molecular motility at a film surface. The largest reported crystals were a few microns in length.

In contrast, the higher solubility of Alq_3 in methanol enhances the diffusion of adsorbed methanol molecules into the amorphous film, thereby enabling "bulk" rather than surface transformations. The imbibed methanol imparts motility to the Alq_3 molecules via a plasticization effect, whereby the T_g of a glassy material is reduced by the presence of low molecular weight additives. Semi-empirical equations based on free-volume considerations predict that a methanol volume fraction of 0.18 in Alq_3 is sufficient to lower T_g to room temperature [18]. The consequent increase in molecular motility enables the Alq_3 to minimize interfacial tension and overall free energy, resulting in dewetting followed by supramolecular assembly of in-plane crystals at room temperature.

Moreover, the large size of the needles is attributed to enhanced transport of Alq_3 resulting from dissolution of Alq_3 in methanol. Since solubility decreases with increasing size, the larger crystalline needles do not dissolve, but rather grow at the expense of the submicron clumps. In the Alq_3/chloroform system studied previously, microcrystallites were observed to dissolve into liquescent strips which experienced capillary flow along the grating grooves [15]. The resulting anisotropic mass transport yielded Alq_3 needles aligned parallel to the grating direction. Although preferential needle orientation on surface-relief gratings was not observed for the Alq_3/methanol system, it should be achievable by adjusting the groove aspect ratio and/or the surface chemistry [16].

5. Conclusions

We have demonstrated the supramolecular assembly of isolated, in-plane Alq_3 crystalline needles via room temperature solvent-vapor exposure of initially amorphous thin films. The large size (tens of microns in length) of the crystals results from enhanced mass transport due to the solubility of Alq_3 in methanol. The formation of much larger (millimeter-scale), oriented crystals should be possible using appropriate surface-relief and surface chemistry. Beyond this, an understanding of the crystal seeding process is necessary to enable placement of organic crystals at specified locations on a substrate for practical device fabrication. Organic crystalline needles generated via solvent-vapor exposure may have enhanced charge carrier mobilities necessary for organic electronic applications such as low-voltage field-effect transistors and high-efficiency solar cells, or non-linear optical properties required for organic optoelectronic devices such as modulators, optical filters, and polarization rotators.

6. References

[1] F.R. Lipsett, Can. J. Phys., vol. 35, pp. 284-298, 1957.

[2] M. Pope, H.P. Kallmann, and P. Magnante, J. Chem. Phys., vol. 38, pp. 2042-2043, 1963.

[3] V. Podzorov, V.M. Pudalov, and M.E. Gershenson, Appl. Phys. Lett., vol. 82, pp. 1739-1741, 2003.

[4] F. Pan, K. McCallion, and M. Chiappetta, Appl. Phys. Lett., vol. 74, pp. 492-494, 1999.

[5] C.D. Dimitrakopoulos and P.R.L. Malenfant, Adv. Mater., vol. 14, pp. 99-117, 2002.

[6] A.M. Hor and R.O. Loutfy, Thin Solid Films, vol. 106, pp. 291-301, 1983.

[7] F. Iwatsu, J. Cryst. Growth, vol. 71, pp. 629-638, 1985.

[8] M. Brinkmann, J.C. Wittmann, C. Chaumont, and J.J. Andre, Thin Solid Films, vol. 292, pp. 192-203, 1997.

[9] J.C. Conboy, E.J.C. Olson, D.M. Adams, J. Kerimo, A. Zaban, B.A. Gregg, and P.F. Barbara, J. Phys. Chem. B, vol. 102, pp. 4516-4525, 1998.

[10] C.W. Tang and S.A. Vanslyke, Appl. Phys. Lett., vol. 51, pp. 913-915, 1987.

[11] K. Naito and A. Miura, J. Phys. Chem., vol. 97, pp. 6240-6248, 1993.

[12] E.M. Han, L.M. Do, N. Yamamoto, and M. Fujihira, Thin Solid Films, vol. 273, pp. 202-208, 1996.

[13] J.F. Moulin, M. Brinkmann, A. Thierry, and J.C. Wittmann, Adv. Mater., vol. 14, pp. 436-439, 2002.

[14] F. Toffolo, M. Brinkmann, O. Greco, F. Biscarini, C. Taliani, H.L. Gomes, I. Aiello, and M. Ghedini, Synth. Met., vol. 101, pp. 140-141, 1999.

[15] D.J. Mascaro, M.E. Thompson, H.I. Smith, and V. Bulović, Org. Electron., accepted 2005.

[16] R. Seemann, M. Brinkmann, E.J. Kramer, F.F. Lange, and R. Lipowsky, Proc. Natl. Acad. Sci. U. S. A., vol. 102, pp. 1848-1852, 2005.

[17] M. Brinkmann, G. Gadret, M. Muccini, C. Taliani, N. Masciocchi, and A. Sironi, J. Am. Chem. Soc., vol. 122, pp. 5147-5157, 2000.

[18] J. Bicerano, Prediction of Polymer Properties, New York: Marcel Dekker, Inc., 1996.